Seismic Performance of Cellular Lightweight Concrete Block Panels as Infilled Wall in RC Frames Due to Cyclic Lateral Loading

Yusran Londong Salu
Civil Engineering Department, Faculty of Engineering, Hasanuddin University, Indonesia
yulosa00@gmail.com

Herman Parung
Civil Engineering Department, Faculty of Engineering, Hasanuddin University, Indonesia
parungherman@yahoo.co.id

Muhammad Wihardi Tjaronge
Civil Engineering Department, Faculty of Engineering, Hasanuddin University, Indonesia
tjaronge@yahoo.co.jp

Rita Irmawaty
Civil Engineering Department, Faculty of Engineering, Hasanuddin University, Indonesia
Rita_irmaway@yahoo.co.id (corresponding author)

Received: 21 July 2024 | Revised: 3 August 2024 | Accepted: 12 August 2024

 DOI: https://doi.org/10.48084/etasr.8444

ABSTRACT

Indonesia experiences frequent earthquakes due to its proximity to seismic faults. Many one- or two-story residential buildings with reinforced concrete frames filled with masonry are severely damaged during moderate to high-magnitude earthquakes. One solution to reduce seismic loads on the structures is the use of Cellular Lightweight Concrete (CLC). The behavior of CLC block panels as an infill wall against lateral cyclic loading is the subject of this experimental investigation. The specimens consist of two Reinforced Concrete (RC) frame models: a CLC block panel used as an infill wall for the RC frame (DB-2) and a reinforced concrete frame (DB-1). This research uses displacement control methods and lateral cyclic loading to evaluate the behavior of wall structures according to the ASTM E2126-02a. The results showed that the strength value of the DB-2 specimen was 29.61% higher than that of the DB-1 specimen. Neither loading nor unloading of the DB-2 specimen caused a decrease in relative stiffness, unlike the DB-1 specimen. This indicates that the DB-2 specimen does not experience a squeezing effect and instead becomes more stable and has improved energy dissipation without losing strength. The results show that bricks, concrete blocks, and other fillers can be replaced with precast CLC panels for reinforced concrete frame walls.

Keywords-cellular lightweight concrete; block panel; lateral cyclic loads

I. INTRODUCTION

Indonesia's geographic location on the Pacific Ring of Fire and the convergence of multiple tectonic plates render the country highly susceptible to seismic activity [1]. It is therefore imperative that earthquake disaster mitigation efforts continue to be carried out in a sustainable manner, with the objective of reducing the risk of losses incurred. In recent decades, sustainable development has emerged as the primary criterion for technical progress, including the construction sector. The majority of sustainability-based innovations result in the production of cement as a construction material. The use of composite Portland cement allows for the incorporation of fly ash, a by-product of coal combustion with a high silica content, thereby reducing CO_2 emissions and the extraction of natural resources [2]. A review of the literature reveals that composite Portland cement can produce concrete with good performance [3-6]. One example of sustainable innovation based on environmentally friendly materials is the use of foam materials in residential homes and high-rise construction systems. The incorporation of foam concrete walls allows structural elements to support less load, which means fewer beams, columns, and foundations are needed, thus reducing the amount of concrete required. Furthermore, the use of foam concrete instead of precast structural elements can lead to a reduction in fuel consumption.

Portland cement, water, fine aggregate, and foam (exclusive of coarse aggregate) comprise the ingredients of CLC. The hardened CLC is of lighter weight than regular concrete due to the numerous small voids created by the foam content. CLC slurry flows readily under its own weight and fills the mold while still fresh due to its optimal consistency [7, 8]. The preliminary research on the use of composite Portland cement in foam concrete indicates that the strength of CLC produced from composite Portland cement is comparable to that of foam concrete made from Ordinary Portland Cement (OPC). Conversely, manufactured housing has gained considerable traction in recent times, driven by the necessity for cost-effective housing solutions. It is essential that manufacturers conduct comprehensive studies and develop a detailed understanding of the behavior of these structures in order to optimize the use of the material [7 -10]. Furthermore, it is essential to guarantee that the design techniques founded upon observed behavior facilitate the implementation and maintenance of structural units. One potential method for developing earthquake-resistant foam concrete walls is the utilization of precast foam concrete panels as infill structures within reinforced concrete frames. The use of precast foam concrete panels as infilled walls for reinforced concrete frames during the installation of walls represents a viable method for overcoming horizontal deviations and enhancing the structural performance of residential and high-rise buildings. The installation of precast foam concrete panels in a vertical orientation on selected building facades results in enhanced structural rigidity, enabling the structure to resist considerable shear forces as it expands. The maintenance of the structure's floor and the prevention of its collapse in the event of an earthquake are functions that are crucial to the overall design of a building. It is possible to provide the requisite horizontal load resistance in an economical manner by placing walls in a strategic manner. In order to reduce seismic vulnerability in single and double-storey residential properties, a series of measures are presented in this research. In addition to the attributes of the reinforced concrete frame, which serves as a reference point for evaluating the seismic resilience of one to two-story dwellings, the filler material used in foam concrete precast panels represents a crucial element that merits consideration. This research examines the correlation between displacement and load in CLC block panels used as infill walls.

II. DESCRIPTION OF SPECIMENS

A. *Material Properties*

The properties of all materials employed in this research, including concrete, mortar, and reinforcing bars, are presented in Tables I and II. It should be noted that the concrete employed in this study comprises CLC, mortar, columns, and lower and upper beams. The properties of each of these materials were evaluated in accordance with relevant international standards. The lower beam is composed of regular concrete with a specified compressive strength of 22.6 MPa and a specified slump range of 12 ± 2 cm. A plain bar is used for the purpose of reinforcing the lower beam, with a diameter of 10 mm (Ø10) for longitudinal reinforcement and 8 mm (Ø8) for shear reinforcement. The objective for the concrete mix design for the columns and upper beams is to achieve a strength of 30 MPa, with a desired slump of 10 ± 2 cm. The 13 mm (*D*13) deformed bar is employed as the longitudinal reinforcement in the column, while the 8 mm (Ø8) plain reinforcement is used for shear reinforcement.

TABLE I. COMPRESSIVE STRENGTH OF MATERIALS USED

Materials	Compressive Strength (MPa)	Standard Method
CLC	7.38	ASTM C39 [11]
Mortar	5.20	ASTM C780 [12]
Column	30.25	ASTM C39 [11]
Lower Beam	22.60	ASTM C39 [11]
Upper Beam	30.25	ASTM C39 [11]

TABLE II. MECHANICAL PROPERTIES OF REINFORCING BARS

Diameter	Stress (MPa)		Classification [13]
	Yield Strength	Ultimate Tensile Strength	
Ø8	377.868	420.964	BjTP 280
Ø10	469.763	598.879	BjTP 280
*D*13	473.744	643.150	BjTS 420A

B. *Specimen Type*

The research specimen comprises two RC frames, one with, and one without infill walls, constructed from lightweight cellular concrete block panels. The RC frames were constructed at a scale of 1:1. Specimen DB-2 is a reinforced concrete frame with lightweight cellular concrete beam panels incorporated into the walls, whereas specimen DB-1 is a reinforced concrete frame without infill walls. Figures 1 and 2 present the specific information pertaining to specimens DB-1 and DB-2, respectively.

C. *Set-up Specimen*

To quantify the extent of deformation during loading, six Linear Variable Differential Transformers (LVDTs) were positioned on both sides of the column. Furthermore, two LVDTs were positioned on the lower beam to regulate the deformation resulting from tensile forces, as shown in Figure 3. The specimens were subjected to horizontal cyclic loading in accordance with the recommendations set forth in ASTM E2126-02a, employing technique B (ISO 16670 Protocol) [14]. Figure 4 shows the configuration of the RC frame with CLC serving as the infill wall specimen. A set of hydraulic actuators was employed to apply cyclic loads to the RC frame. Furthermore, the cycle loads were applied with controlled displacement conditions, with Δm determined by the 2% horizontal deformation of the RC specimen height, as specified by the building design standards of SNI 1726-2019 [15]. The value of Δm was determined to be 40 mm, due to the utilization of a specimen height of 2,000 mm. The loading technique entailed the regulation of displacement and the subdivision of displacement cycles into phases, wherein the rate of displacement was incrementally augmented. The ISO loading is detailed in Table III and illustrated in Figure 5.

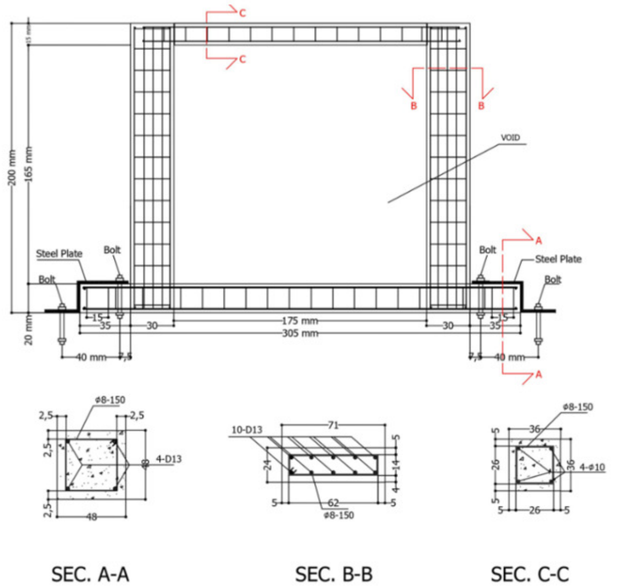

Fig. 1. DB-1 specimen.

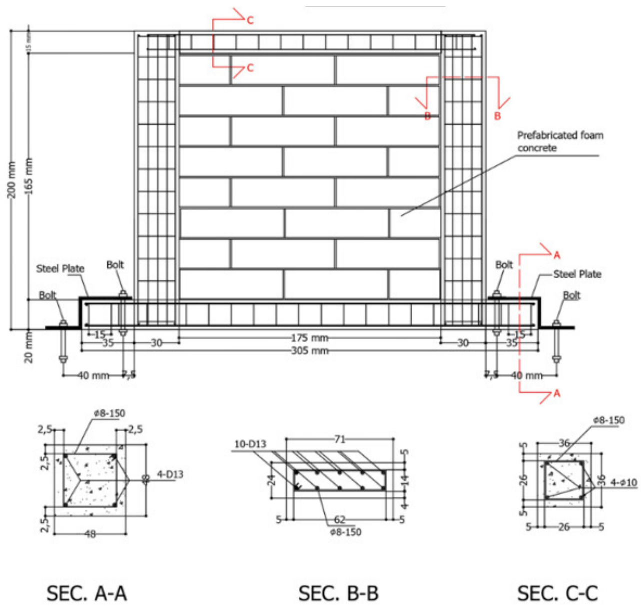

Fig. 2. DB-2 specimen.

III. RESULTS AND DISCUSSION

A. Load-Displacement of DB-1 Specimen

Figure 6 depicts the loop hysteresis curve, which shows the relationship between load and displacement in reinforced concrete frame specimens (DB-1). The DB-1 specimen is used as a control specimen in this study to assess the impact of cyclic loads on CLC when employed as a filler material.

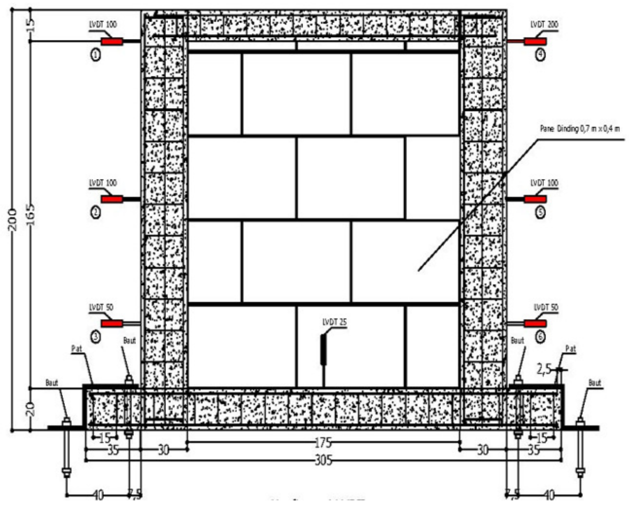

Fig. 3. LVDT configuration.

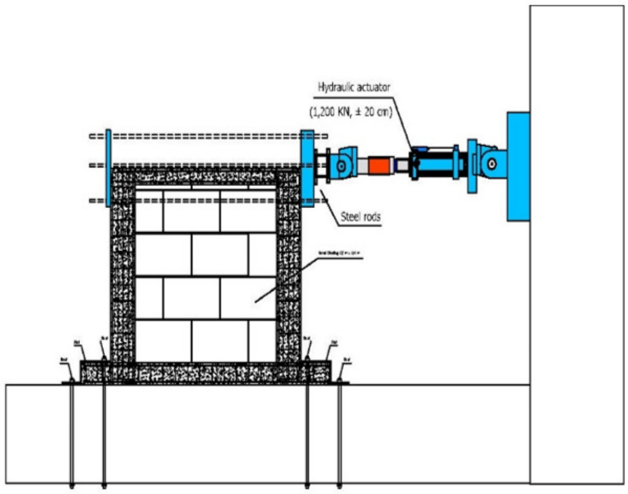

Fig. 4. Setting up test.

TABLE III. LOADING SCHEDULE [14]

Mode	Step	Number of Cycles	Amplitude, % Δm	Drift Ratio %
I	1	1	1.25	0.025
	2	1	2.50	0.05
	3	1	5.00	0.10
	4	1	7.50	0.15
	5	1	10.00	0.20
II	6	3	20.00	0.40
	7	3	40.00	0.80
	8	3	60.00	1.20
	9	3	80.00	1.60
	10	3	100.00	2.00
	11	3	Add increments of 20 until failure	2.40

The DB-1 exhibits linear elastic behavior until reaching a load of 6.93 kN and an amplitude of 7.5% Δm at the onset of compressive loading, as shown by the loop hysteresis curve in Figure 6. In contrast, the DB-1 displays a linear elastic response when subjected to tensile stress, exhibiting a deviation ratio of 7.5% relative to a force of 6.05 kN. As the cyclic load increases, the DB-1's behavior undergoes a gradual transformation due to the influence of the reinforced concrete frame. Upon reaching the post-yielding zone, the specimen transitions from a linear gradient to a nonlinear gradient, exhibiting inelastic behavior. This modification has a direct impact on the lateral stiffness of the specimen.

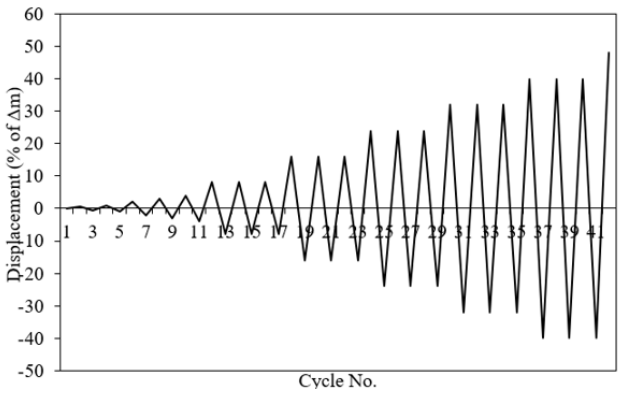

Fig. 5. Loading cycle according to ASTM E2126-02a [14].

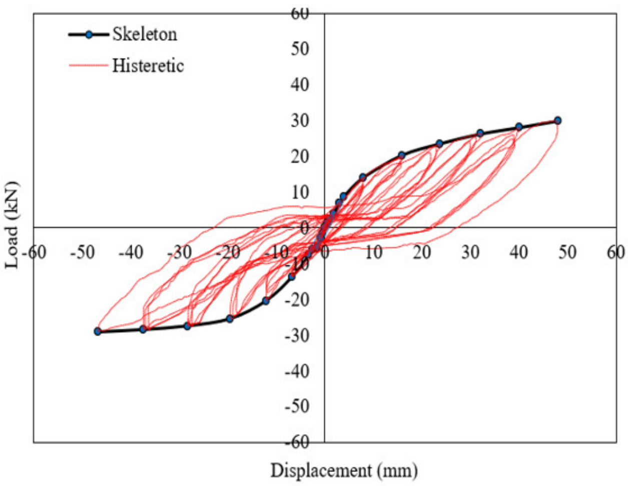

Fig. 6. Load-displacement behavior of DB-1 specimen.

B. *Load-Displacement of DB-2 Specimen*

The hysteresis loop curve, which describes the relationship between load and displacement in the DB-2 specimen, is presented in Figure 7. The DB-2 specimen curve displays a linear increase in load during compressive loading until reaching an amplitude of 40% Δm. Subsequently, the curve undergoes a notable increase until it reaches 100% Δm. Subsequently, the curve exhibits a tendency to level out, with a further rise in load that is negligible. Similarly, when subjected to tensile load, the DB-2 specimen curve demonstrates a consistent and proportional increase in load until it reaches an amplitude of 40% Δm. Subsequently, the curve exhibits a pronounced surge until it reaches an amplitude of 100% Δm. During the course of testing, the DB-2 specimen exhibited a reduction in strength following the attainment of the maximum load at an amplitude of 120% Δm. The resulting hysteresis loop curve is of a broader shape than that of the DB-1 specimen. A reduction in relative stiffness is not discernible in the DB-2 specimen, and no evidence of a pinch effect is observed. This indicates that the DB-2 specimen exhibits greater strength and is capable of absorbing more energy without experiencing a loss in strength.

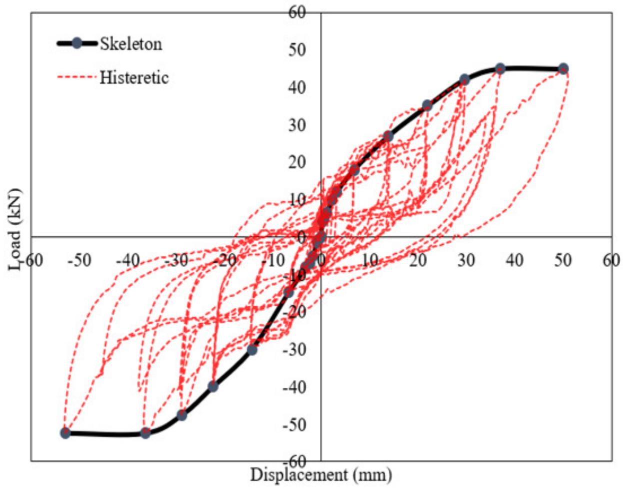

Fig. 7. Load-displacement behavior of DB-2 specimen.

C. *Load-Displacement of All Specimen*

Figure 8 shows that specimen DB-2 demonstrated superior performance to DB-1 during the test, exhibiting a maximum compressive load capacity of 44.88 kN and a tensile load capacity of 52.30 kN, in comparison to DB-1's 29.84 kN and 29.30 kN, respectively.

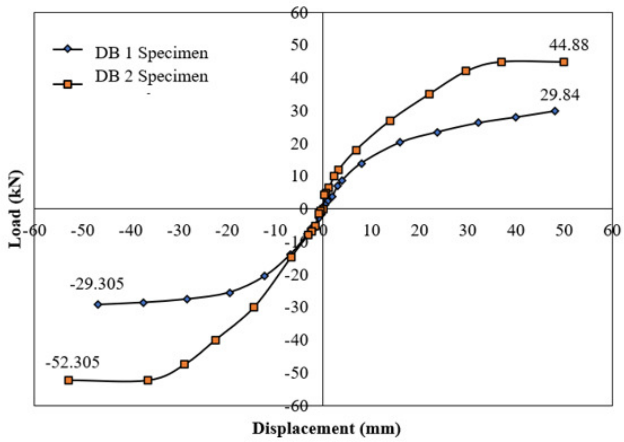

Fig. 8. Load-displacement behavior of all specimens.

Both specimens demonstrated robust performance and did not fail. Authors in [16] observed a 62.5% increase in the ultimate load of RC frames filled with autoclave aerated concrete brick masonry compared to reinforced concrete frames without any infill. Furthermore, authors in [17] highlighted the impact of infill panels on the seismic behavior of the structure by emphasizing the increased acceleration spectrum resulting from the enhanced stiffness of the infill structure.

D. Failure Mechanism

This section presents an overview of the failure processes that occur in wall specimens during lateral cyclic testing, with a particular focus on in-plane failure. The failure mechanisms observed encompass a range of cracking patterns in concrete, cellular lightweight concrete materials, and reinforced concrete column portal systems. Figure 9 depicts the failure mechanism of the DB-1 specimen. The initial fracture occurred in the DB-1 specimen column when it was subjected to a tensile force of 3.79 kN and an amplitude change in mass of 5%. During the compression process, the initial failure occurred at the connection point between the beam and column, with a deformation of 7.5%Δm and a load of 6.93 kN. The crack is observed to emerge at a distance of 156 centimeters from the front of the column on the lower side of the beam. It is probable that the fracture is situated in the vicinity of the column and beam joint, within the plastic hinge region. The distribution of the crack along the column is relatively homogeneous. Given that the fracture path is at a right angle to the direction of the load, the fracture is categorized as a flexural crack.

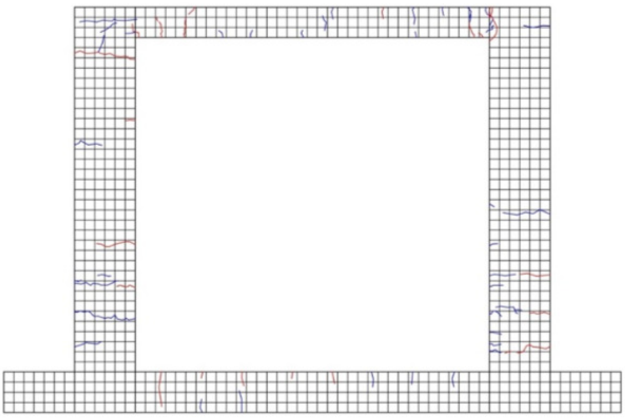

Fig. 9. Failure mechanism of DB-1 specimen.

The observed crack patterns suggest that the DB-1 specimen is capable of efficiently transmitting force. Tensile loading results in the formation of new bending cracks on the upper surface of the beam. As the cyclic horizontal force intensifies, additional fractures emerge. The fissure subsequently expands and stretches towards the periphery of the beam, ultimately leading to a vertical fracture that spans the entire width of the beam. The initial bending crack on the upper side of the beam will intersect with a bending crack on the lower side, resulting in the formation of additional cracks around the entire circumference of the beam. Furthermore, additional flexural cracks will be generated outside the plastic hinge region when the load exceeds the yield point. The fracture expands in proportion to the increase in the applied load. During the dismantling of the DB-1 specimen, it was observed that the widening of the fractures occurred as a result of the yielding of the longitudinal reinforcement. Let us consider a scenario in which a load in the positive direction exceeds its maximum capacity or post-peak response amplitude by 100% of the change in mass (Δm). In such an instance, it can be inferred that the load has exceeded the maximum capacity of the beam-column section, resulting in an average decrease of approximately 20%. Moreover, evidence of delamination is present on the underside of the top beam.

Following meticulous examination and analysis, it was determined that flexural fractures emerged in pivotal locations in close proximity to the column's surface. It is noteworthy that the specimens typically reached their maximum bending strength before experiencing shear failure. The crack in the plastic hinge area of the lower beam and column widens, extending towards the middle of the lower or upper beam and eventually reaching the top of the specimen when the amplitude reaches 120% Δm. This phenomenon is accompanied by an increase in lateral loads. The RC frame portal is affected by spalling and significant flexural cracks, rendering reinforcement and repair efforts ineffective and costly. The number of fissures at the juncture of beams and columns is increasing at a gradual but consistent rate. Moreover, there was an increase in the number and size of cracks in the lower beam, with fissures also emerging in the plastic hinge region. Figure 10 shows the failure process seen in specimen DB-2.

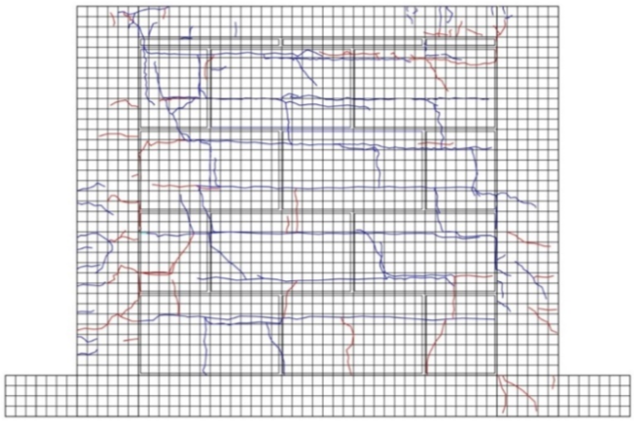

Fig. 10. Failure mechanism of DB-2 specimen.

The brittleness of the infill wall, comprising cellular lightweight concrete precast panels, resulted in the specimen DB-2 displaying a multitude of cracks and, subsequently, a collapse when subjected to in-plane stresses. The initial fracture in the DB-2 sample occurred in the infill wall made of cellular lightweight concrete as a result of tensile forces exerted at a load of 5.13 kN and an amplitude of 5.0% Δm. Furthermore, the beam-column joints and the mortar joints between the infill walls, which were constructed from precast cellular lightweight concrete panels, also exhibited cracking. Tensile loads resulted in the formation of cracks with an amplitude of 40.0% Δm and a load of 13.85 kN. The crack is observed to emerge at a distance of 185 cm from the strong floor on the lower side of the bottom beam. It is postulated that the fracture is located in the plastic hinge region surrounding the connection between the beam and the column. The cracks in the beam are distributed in a uniform manner. The fracture pattern is classified as a flexural crack due to its perpendicular alignment with the direction of the applied load. The observed crack pattern indicates that the DB-2 specimen exhibits efficient force transmission capabilities. As the frequency of cycles and the load response intensify, the quantity of cracks in the plastic hinge region surrounding the beam-column connection likewise increases. Subsequently, the crack propagated in a direction towards the corner of the infill wall, specifically the precast cellular lightweight concrete panel. The crack continued to grow until it reached an amplitude of 80.0% Δm at the midpoint and end of the specimen. Additionally, the incident is marked by the deterioration of the filling walls, particularly in areas along the seams between them.

The strain readings obtained from the strain gauge attached to the rebar indicate that the longitudinal reinforcement in the plastic connection area is beginning to yield, leading to the formation of a plastic hinge mechanism at the beam-column connection. Additionally, it was observed that shear crack patterns emerged, aligning with the direction of the applied load. Moreover, the crack propagation initiates at the point of origin and intersects with the infill wall, specifically at the mortar-infill wall interface. In the subsequent amplitude test, which concluded with an amplitude of 100% Δm, no additional cracks were observed, but the preexisting cracks exhibited expansion. This phenomenon occurs when longitudinal reinforcement is applied to the joint region, thereby forming a plastic hinge mechanism in the beam-column connection. The plastic is currently undergoing dissolution. The formation of shear fractures is contingent upon the alignment of cracks with the direction of the applied load. In addition to the infill wall, the width of the cracks increases in the layer where the infill wall and mortar intersect. Furthermore, the fragmented components of the cellular lightweight concrete filler material demonstrate an inadequate response from the mortar at their joints, resulting in excessive and increasing displacement when subjected to in-plane loads. The lack of adequate bonding between the infill wall and the RC frame contributes to the infill wall's poor in-plane stability, which is further compromised by the mortar in the joints between the infill components. A visible deterioration is evident in the seams between the infill wall and the mortar. The infill wall sustained immediate damage due to the failure of the mortar, which serves as a connecting element between the infill wall and the surrounding structure, as shown in Figure 11.

IV. CONCLUSIONS

The results of the experimental investigation on two Reinforced Concrete (RC) frames, one filled with lightweight cellular concrete block panel walls and the other without, were derived from an analysis of the load and displacement correlations. In conclusion, the findings of the investigation can be summarized as follows:

- The use of prefabricated cellular lightweight concrete block panels as infill walls demonstrates favorable structural behavior with regard to the acceptance of earthquake loads, as compared to frames that lack infill walls. This is evidenced by an increase in compressive load of 50.40% and an increase in tensile load of 78.50% in reinforced concrete frame walls.

Fig. 11. Failure mechanism in joints between CLC materials of DB-2 specimen.

- In most cases, walls in structures serve a function that is supportive, divisional, or separative, rather than a structural one. Nevertheless, research findings suggest that prefabricated Cellular Lightweight Concrete (CLC) panels used as infill materials demonstrate a robust structural response to seismic stress.
- Prefabricated CLC panels can be employed in the construction of walls with RC frames as an alternative to traditional infill materials such as bricks and concrete blocks. Furthermore, CLC can be used as a roofing material in a variety of industrial and agricultural applications, including industrial buildings and warehouses, septic tank walls, water storage tanks, drains, and agricultural product storage warehouses.
- Future research will concentrate on the advancement of CLC panel technology with the objective of enhancing earthquake resistance in high-rise buildings and improving their architectural and constructional aspects.

REFERENCES

[1] L. Hamzah, N. Puspito, and F. Imamura, "Tsunami Catalog and Zones in Indonesia," *Journal of Natural Disaster Science*, vol. 22, no. 1, pp. 25–43, Jan. 2000, https://doi.org/10.2328/jnds.22.25.

[2] J. Deja, A. Uliasz-Bochenczyk, and E. Mokrzycki, "CO2 emissions from Polish cement industry," *International Journal of Greenhouse Gas Control*, vol. 4, no. 4, pp. 583–588, Jul. 2010, https://doi.org/10.1016/j.ijggc.2010.02.002.

[3] I. F. Al-Mulla, A. S. Al-Ameeri, A. S. Al-Rihimy, and T. S. Al-Attar, "Elasticity and Load-Displacement Behavior of Engineered Cementitious Composites produced with Different Polymeric Fibers," *Engineering, Technology & Applied Science Research*, vol. 14, no. 1, pp. 13026–13032, Feb. 2024, https://doi.org/10.48084/etasr.6731.

[4] E. F. Irassar, V. L. Bonavetti, G. P. Cordoba, V. F. Rahhal, C. C. Castellano, and H. A. Donza, "Performance of Composite Portland Cements with Calcined Illite Clay and Limestone Filler Produced by Industrial Intergrinding," *Minerals*, vol. 13, no. 2, Feb. 2023, Art. no. 240, https://doi.org/10.3390/min13020240.

[5] N. Bheel, M. A. Jokhio, J. A. Abbasi, H. B. Lashari, M. I. Qureshi, and A. S. Qureshi, "Rice Husk Ash and Fly Ash Effects on the Mechanical Properties of Concrete," *Engineering, Technology & Applied Science Research*, vol. 10, no. 2, pp. 5402–5405, Apr. 2020, https://doi.org/10.48084/etasr.3363.

[6] M. A. Caronge, M. W. Tjaronge, H. Hamada, and R. Irmawaty, "Effect of water curing duration on strength behaviour of portland composite cement (PCC) mortar," *IOP Conference Series: Materials Science and Engineering*, vol. 271, no. 1, Nov. 2017, Art. no. 012018, https://doi.org/10.1088/1757-899X/271/1/012018.

[7] Y. H. M. Amran, N. Farzadnia, and A. A. Abang Ali, "Properties and applications of foamed concrete; a review," *Construction and Building Materials*, vol. 101, pp. 990–1005, Dec. 2015, https://doi.org/10.1016/j.conbuildmat.2015.10.112.

[8] V. Lesovik *et al.*, "Improving the behaviors of foam concrete through the use of composite binder," *Journal of Building Engineering*, vol. 31, Sep. 2020, Art. no. 101414, https://doi.org/10.1016/j.jobe.2020.101414.

[9] Y. Sunarno, M. W. Tjaronge, and R. Irmawaty, "Preliminary study on early compressive strength of foam concrete using Ordinary Portland Cement (OPC) and Portland Composite Cement (PCC)," *IOP Conference Series: Earth and Environmental Science*, vol. 419, no. 1, Jan. 2020, Art. no. 012033, https://doi.org/10.1088/1755-1315/419/1/012033.

[10] Sahiruddin, M. W. Tjaronge, and R. Irmawaty, "Physical behavior of foam concrete constructed with blended cement and polyolefin fiber," in *1st International Conference on Technology, Informatics, and Engineering*, Malang, Indonesia, Jul. 2022, vol. 2453, Art. no. 020026, https://doi.org/10.1063/5.0096707..

[11] *ASTM C39/C39M-21: Standard Test Method for Compressive Strength of Cylindrical Concrete Specimens*. West Conshohocken, PA, USA: ASTM International, 2003.

[12] *ASTM C780-20:* S*tandard Test Method for Preconstruction and Construction Evaluation of Mortars for Plain and Reinforced Unit Masonry*. West Conshohocken, PA, USA: ASTM International, 2012.

[13] SNI 2052:2017: Baja Tulangan Beton. Indonesia: SNI 2017.

[14] *ASTM E2126-19 : Standard Test Methods for Cyclic (Reversed) Load Test for Shear Resistance of Vertical Elements of the Lateral Force Resisting Systems for Buildings.* ASTM International. West Conshohocken, PA,USA, 2019.

[15] *SNI 1726:2019: Tata Cara Perencanaan Ketahanan Gempa untuk Struktur Bangunan Gedung dan Non-gedung*. Indonesia: SNI, 2019.

[16] P. Jagadeesan *et al.*, "Study on Performance of Infilled Wall in an RC-Framed Structure Using a Reinforcing Band," *Advances in Materials Science and Engineering*, vol. 2022, no. 1, 2022, Art. no. 8643959, https://doi.org/10.1155/2022/8643959.

[17] A. De Angelis and M. R. Pecce, "The Role of Infill Walls in the Dynamic Behavior and Seismic Upgrade of a Reinforced Concrete Framed Building," *Frontiers in Built Environment*, vol. 6, Dec. 2020, Art. no. 590114, https://doi.org/10.3389/fbuil.2020.590114.